Acta Cryst. (1996). D52, 18–29

Structure of Bovine Pancreatic Trypsin Inhibitor at 125 K: Definition of Carboxyl-Terminal Residues Gly57 and Ala58

SEAN PARKIN[a]*† BERNHARD RUPP[b] AND HÅKON HOPE[a]*

[a]*Department of Chemistry, University of California, Davis, CA 95616, USA, and* [b]*Biology and Biotechnology Research Program, L-452, Lawrence Livermore National Laboratory, Livermore, CA 94550, USA*

(*Received 31 March 1995; accepted 27 June 1995*)

Abstract

The structure of bovine pancreatic trypsin inhibitor has been refined to a resolution of 1.1 Å against data collected at 125 K. The space group of the form II crystal is $P2_12_12_1$ with $a=75.39(3)$, $b=22.581(7)$, $c=28.606(9)$ Å (*cf.* $a=74.1$, $b=23.4$, $c=28.9$ Å at room temperature). The structure was refined by restrained least-squares minimization of $\sum w(F_o^2-F_c^2)^2$ with the *SHELXL*93 program. As the model improved, water molecules were included and exceptionally clear electron density was found for two residues, Gly57 and Ala58, that had been largely obscured at room temperature. The side chains of residues Glu7 and Arg53 were modelled over two positions with refined occupancy factors. The final model contains 145.6 water molecules distributed over 167 sites, and a single phosphate group disordered over two sites. The root-mean-square discrepancy between Cα atoms in residues Arg1–Gly56 at room and low temperatures is 0.4 Å. A comparison of models refined with anisotropic and isotropic thermal parameters revealed that there were no significant differences in atomic positions. The final weighted *R*-factor on F^2 (wR_2) for data in the range 10–1.1 Å was 35.9% for the anisotropic model and 40.9% for the isotropic model. Conventional *R* factors based on *F* for $F>4\sigma(F)$ were 12.2 and 14.6%, respectively, corresponding to 16.1 and 18.7% on all data. These large *R*-factor differences were not reflected in values of *R*(free), which were not significantly different at 21.5(5) and 21.8(4)%, respectively. These results, along with the relatively straightforward nature of the refinement, clearly highlight the benefits of low-temperature data collection.

1. Introduction

Bovine pancreatic trypsin inhibitor (BPTI), ($M_r=6500$, 58 amino acids) has been the subject of intense scrutiny for many years. The structures of three crystalline forms of native BPTI and various mutants are present in the Brookhaven Protein Data Bank (Bernstein *et al.*, 1977). The first (form I, in space group $P2_12_12_1$) was solved by Huber, Kukla, Rühlmann, Epp & Formanek (1970) by multiple isomorphous replacement on data to a resolution of 2.5 Å. This structure was further refined to a resolution of 1.5 Å by Deisenhofer & Steigemann (1975). A second form (also in space group $P2_12_12_1$) diffracts X-rays to a resolution of at least 1 Å, and has been refined in a number of studies (Walter & Huber, 1983; Wlodawer, Walter, Huber & Sjölin, 1984*a*,*b*; Eigenbrot, Randal & Kossiakoff, 1991). Form II BPTI has also been refined against 2.0 Å resolution neutron diffraction data (Wlodawer *et al.*, 1984*a*,*b*). The structure of a third form, in space group $P2_12_12$ was reported by Wlodawer, Nachman, Gilliland, Gallagher & Woodward (1987), at room temperature to a resolution of 1.7 Å.

As a result of the relatively high quality of structural models available, BPTI has been used as a model to interpret structural information obtained by other techniques. For example, BPTI played a role in the development of two-dimensional NMR (Wüthrich, Wider, Wagner & Braun, 1982), computer simulations of protein dynamics (Levitt, 1981, 1983; Brooks & Karplus, 1983), and structure prediction based on amino-acid sequence (Takanaga & Scheraga, 1975; Levitt & Warshel, 1975).

The resolution limit attainable in diffraction studies from form II crystals of BPTI places it in an exclusive class of small proteins that have been refined at true atomic resolution. This group includes crambin (Teeter & Hendrickson, 1979), some rubredoxins (Pierrot *et al.*, 1976; Watenpaugh, Sieker & Jensen, 1979; Dauter, Sieker & Wilson, 1992), and avian pancreatic polypeptide (Glover *et al.*, 1993). Despite the high resolution attainable with native BPTI crystals, room-temperature data collection to date has failed to produce interpretable electron density for the carboxyl terminus residues Gly57 and Ala58. Diffraction data from a Tyr35Gly mutant gave good electron density at these positions (Housset, Kim, Fuchs, Woodward & Wlodawer, 1991*a*,*b*). However, crystals of this mutant grow in space group $P4_22_12$ and are not directly comparable to form II native crystals. In addition to the problems associated with Gly57 and Ala58, the S atom of Met52 has previously been found to be oxidized in room-temperature studies (Eigenbrot *et al.*,

† Present address: Biology and Biotechnology Research Program, L-452, Lawrence Livermore National Laboratory, Livermore, CA 94550, USA.

1991). Since Met52 is not oxidized in the biologically active state, this observed effect must have occurred as a result of X-ray irradiation.

The amount of information that can be extracted from low-temperature data is generally greater than that for room-temperature data. Reduced thermal motion effectively enhances the contrast in electron-density maps, making them easier to interpret. Perhaps the greatest advantage of reduced temperatures, however, is the postponement of the detrimental effects of radiation damage and the elimination of the need for cumbersome capillary mounts (Hope, 1988). In the 1 Å structure of BPTI reported by Wlodawer *et al.* (1984*a*,*b*) for example (5PTI), 18 different crystals were needed to obtain a complete data set. Each crystal was irradiated until the intensity of check reflections had dropped by ~10% of their initial values. Structural information derived from this room-temperature data set thus represents an average over not only the 18 crystals used, but also any structural damage incurred during exposure.

Crystals of BPTI were among the first macromolecular crystals to be cooled in the crystallography laboratory at UC Davis (Hope, 1988). In those experiments, three form II crystals of BPTI were flash cooled to 125 K in oil without suffering any ill effects. A data set extending to 1.1 Å resolution was collected from one of the crystals. Prior to the present study, this data set had not been used in structure refinement. In light of the problems associated with the room-temperature refinements and the surprisingly anisotropic unit-cell contraction, the need for a careful refinement of the structure against low-temperature data was apparent.

2. Materials and methods

2.1. *Crystallization*

Crystals of BPTI form II can be prepared following the method described by Walter & Huber (1983). Briefly, 5 ml of 0.5 *M* K/Na phosphate buffer (pH = 10.0) are added to 20 ml of a 50 mg ml^{-1} solution of the protein in water. This solution is equilibrated by vapour diffusion with a reservoir of the same phosphate buffer. Large crystals form after a few weeks. The crystal used for data collection in this work was obtained from Wayne Hendrickson.

2.2. *Data collection and processing*

Form II crystals of BPTI have the symmetry of space group $P2_12_12_1$. The cell dimensions at 125 K were $a = 75.39(3)$, $b = 22.581(7)$, $c = 28.606(9)$ Å, volume = 48 698 (29) Å^3. Cooling the crystal to 125 K resulted in a volume decrease of about 3% compared to the room-temperature cell given by Walter & Huber (1983) ($a = 74.1$, $b = 23.4$, $c = 28.9$ Å, volume = 50 111 Å^3). Such contractions are normal for molecular crystals upon cooling (Hartmann *et al.*, 1982; Hope, 1988). The lengthening of the *a* axis, however, gives an indication of a more profound structural change accompanying the cooling process. A crystal of approximate dimensions 1.00 × 0.40 × 0.25 mm was mounted on a straight glass fibre using the oil-drop technique (Hope, 1988). The crystal was placed in the (initially deflected) cold stream path of a modified Syntex LT-1 low-temperature apparatus attached to a Syntex $P2_1$ diffractometer. Once the crystal was in place, rapid cooling was effected by quickly removing the obstruction. Diffraction maxima base-to-base scan widths were all within 1° in ω. Intensities were observed to decrease rapidly with increasing diffraction angle. As a result of the observed fall-off in intensity, the data set was collected in three shells over five days, from $0° < 2\theta < 60°$ at 58.6° min^{-1} (Hope & Nichols, 1981) at 10° min^{-1} for $60° < 2\theta < 90°$ and at 6° min^{-1} for $2\theta > 90°$. Analysis of check reflections, and remeasurement of the first 7000 data points, showed only small random fluctuations, indicating that the effects of radiation damage on the intensity measurements had been eliminated. Data-collection statistics are given in Table 1.

Table 1. *Summary of data-collection statistics for BPTI*

Crystal system	Orthorhombic
Space group	$P2_12_12_1$
Temperature (K)	125
a (Å)	75.39 (3)
b (Å)	22.581 (7)
c (Å)	28.606 (9)
Z	4
Volume (Å^3)	48698 (29)
Diffractometer	Syntex $P2_1$
Radiation	Sealed tube Cu $K\alpha$
Monochromator	Graphite crystal
Scan type	2θ–θ
Scan speed (° min^{-1})	58.6 ($0 < 2\theta < 60°$), 10 ($60 < 2\theta < 90°$), 6 ($2\theta > 90°$)
Check reflections	2 measured every 400 and remeasurement of the first 7000 data points, <2% variation
Measured	28980
Independent reflections	20781 [$11485 > 2\sigma(I)$]
Background measurement	Stationary counter, stationary crystal, at beginning and end of scan, each for half the total scan time.

2.3. *Solution and refinement*

The structure was refined using β and γ test versions of *SHELXL*92 and the final release version, *SHELXL*93 (Sheldrick, 1992, 1993) running on a variety of computers including a DEC Vaxstation 3100 M38, Silicon Graphics Indigo R4000, and a Cray Y-MP. Initially, model rebuilding was carried out by analysis of discrete electron-density peaks found by *SHELXL*92. In the later stages of refinement, model analysis and rebuilding were carried out with the program *Xfit* from the *XtalView* package (McRee, 1992) on a Silicon Graphics Indigo R4000. The following description of model construction and restraint imposition is rather

detailed, and is intended to illustrate the ease with which the ostensibly small-molecule refinement program *SHELXL92/3* (Sheldrick, 1992, 1993) can be used for macromolecule structures.

Starting parameters were taken from the 1.0 Å resolution room-temperature coordinate set 5PTI (Wlodawer *et al.*, 1984*b*). Prior to the first round of refinement, the input parameters were modified as follows. (i) All reference to disorder was removed and the major conformations of disordered groups were assigned full occupancy. (ii) H atoms were removed. (iii) isotropic thermal parameters were halved, converted from '*B*' format to '*U*' format ($B = 8\pi^2 U$), and rounded to the nearest 0.01 Å^2. (iv) The geometry of each amino-acid residue and the distances and angles between them were restrained according to the specific schemes of *SHELXL92/3* to conform to the 'known' geometries given by Engh & Huber (1991). Bond lengths and angles were restrained by loosely tying interatomic distances (restraint 'DFIX' in *SHELXL92/3*), and planarity conditions were applied (restraints 'FLAT' and 'CHIV', the latter can be used to set the 'chiral volume' of an atom to zero). In disordered residues, the geometries of each component were constrained to sum to unity. Where necessary, coordinates and thermal parameters for a given atom from each component were tied to the same coordinates (constraint 'EXYZ', equal x, y, z) and thermal parameter (constraint 'EADP', equal atomic displacement parameter). Thermal parameters of adjacent atoms were restrained to similar values ('SIMU' restraint), and in the refinement runs with anisotropic thermal parameters, the U_{ij} were lightly restrained to remain approximately isotropic (restraint 'ISOR'). Rigid groups were subject to a rigid-bond condition ('DELU' restraint) in which the components U_{ij} along a given interatomic vector are made similar. The relative strength of each restraint was determined by a 'simulated' estimated standard deviation. All 63 water molecules in the 5PTI file were retained in the initial model. Some of the geometric restraints were later relaxed by tying equivalent distances to the same refinable variable.

Refinement proceeded in rounds of least-squares minimization of $\sum w(F_o^2 - F_c^2)^2$, followed by analysis of structural features and critical assessment of peak-list tables produced by the peak-picking routine in *SHELXL92*. All data with $I > 0$ were used from the outset. Atoms were removed if their coordinates became inconsistent with known geometries and if their thermal parameters became too high. The criteria used for rejection depended to a large extent on the type and location of the atom in question. Those belonging to the protein molecule were deemed suspect if their U values went above about 0.3–0.4 Å^2, depending on whether alternative positions could be found in electron-density maps. Water molecules were either removed altogether or were split over two sites following similar, though less strict, considerations. Extreme care was taken in interpreting refinement results as true structural features because of the tendency of the least-squares process to 'remember' false features in non-centrosymmetric space groups.

The first six rounds of refinement each consisted of 24 cycles of blocked full-matrix least-squares minimization of $\sum w(F_o^2 - F_c^2)^2$, corresponding to six cycles of full-matrix refinement. After the first round, there was a substantial drop in the R value, from about 45 to 30% [based on F calculated for $F > 4\sigma(F)$]. Restraints on the geometries of each amino acid and the peptide linkages were tightened, the water structure was completely rebuilt from a difference map, and a model for disorder at Met52 was introduced. Residue Ala58 had become severely distorted. As there was no recognizable electron density in the difference map, it was altered manually to fit the geometry of alanine. Following round 2, the R factor fell to 26.8%. The three disulfide linkages were now very well defined, and anisotropic thermal parameters were included for the six S atoms. Disorder was modelled at Arg17 and a second phosphate group was identified. Occupancy factors for the two phosphates were fixed at 50% each. Residue Ala58 was adjusted, and the water structure was rebuilt, resulting in 50 new water positions, though some of the old ones were removed. After round 3, the R factor dropped to 22.4%. Residues Gly57 and Ala58 were removed from the model because their thermal parameters were very high and no readily interpretable electron density could be found for them. The side chain of Met52 was also rebuilt. Round 4 converged with an R factor of 20.8%. At this point, in order to remove possible bias (from always refining the same parameters together), the full-matrix blocks were reorganized (statement 'BLOC' in *SHELXL92/3*). The water structure was rebuilt and residue Gly56 was given zero weight. Rounds 5 and 6 gave only negligible reduction in R, which dropped to 20.2%. Careful analysis of a difference Fourier map indicated a sequence of electron-density peaks and 'water molecules' that were in positions consistent with the geometries of the omitted residues Gly56, Gly57 and Ala58. These new positions were included in the model at full occupancy. Thermal parameters for some atoms in the side chain of Arg42 had become quite large ($U > 0.4$ Å^2), and the affected atoms were removed. Two new probable water molecules were also included. The seventh round of refinement consisted of 16 cycles of blocked full-matrix least-squares refinement (equivalent to four full-matrix cycles) and led to a slightly reduced R value of 20.1%. This small decrease aroused suspicion, as a larger drop had been anticipated in view of the newly resurrected C-terminus residues. After a thorough analysis of the coordinate file, a (typographical) restraint error was found that attempted to force a distance of about 20 Å to be the same as a C—S bond. This error was corrected, parts of the water structure were rebuilt, and disorder was modelled for the side chains of

Glu7, Arg42 and Arg53. For the eighth round of refinement, the γ-test version of *SHELXL*92 (Sheldrick, 1992) was used. An anti-bumping condition ('BUMP' restraint) was imposed on the water molecules to prevent them from approaching too close to one another or to atoms of the protein molecule. A means of modelling diffuse solvent water by Babinet's principle (Langridge *et al.*, 1960; Driessen *et al.*, 1989) was introduced (command 'SWAT' in *SHELXL*92/3). A total of 24 cycles of least-squares refinement, using a conjugate-gradient algorithm to minimize $\sum w(F_o^2 - F_c^2)^2$, were performed in four separate runs. Small adjustments were made to the less well defined amino-acid side chains and the water structure, and convergence was reached with $R = 17.5\%$ [based on $F > 4\sigma(F)$]. At this stage all non-H protein atoms were present, no new features could be seen in a difference Fourier map, and so the structure was assumed to be essentially complete. H atoms were included using a 'riding' model at calculated positions with fixed isotropic thermal parameters. Methyl and amine groups were placed in staggered conformations and hydroxyl protons were placed in positions that formed the most plausible hydrogen-bonding network. After refinement to convergence, the experimental data were corrected for absorption effects (transmission factors ranged from 0.44 to 0.70) using the program *XABS*2 (Parkin, 1993; Parkin, Moezzi & Hope, 1995). Further refinement lowered the R factor by 2.5 percentage points, but only minor adjustments were made by the least-squares process. In an attempt to flatten out artifacts in the difference electron-density surface so that any missing structural features could be identified, restrained anisotropic thermal parameters were calculated for all well ordered non-H atoms. Although the observation-to-parameter ratio of 3.6:1 resulting from this treatment was on the low side, there were no adverse effects on the structure. Some of the water molecules, however, were subsequently split over two sites with halved occupancy factors (at the suggestion of *SHELXL*92) and the thermal parameters of the C atom of Arg20 had to be made isotropic again. Amino-acid residues with high thermal parameters were selectively omitted from the model and re-introduced from difference Fourier maps. No new atoms were identified in these maps, but disorder models for all side chains apart from Glu7 and Arg53 were eventually removed. Subsequent analysis of Fourier maps using *XtalView* (McRee, 1992) based on a variety of coefficients ($F_o - F_c$, F_o, $2F_o - F_c$, $5F_o - 4F_c$) failed to reveal convincing evidence of multiple configurations in any side chains other than those of Glu7 and Arg53.

The R(free) statistic (Brünger, 1992, 1993), which has been proposed as an unbiased indicator of information content (and hence of residual phase error) showed little change after anisotropic refinement, in contrast to the conventional R factor, which was substantially lower for the model with anisotropic thermal parameters.

Table 2. *Summary of model rebuilding and refinement progress*

Round	Cycles	wR_2 (%)	R_1 (%)	Changes made after each run
1	6*	68.0	30.0	Peptide linkages fixed, restraints tightened, water structure rebuilt, disorder at Met52 modelled, Ala58 fixed
2	6*	63.5	26.8	Disorder at Arg17 and phosphate modelled, Cys S_γ atoms made anisotropic, Ala58 rebuilt, 50 new waters added, some old ones removed
3	6*	57.4	22.4	Gly57 and Ala58 removed, Met52 rebuilt
4	6*	54.3	20.8	Full-matrix blocks reorganized, Gly56 removed, water structure rebuilt
5	6*	54.3	20.6	Gly56, Gly57, Ala58 built up from difference map peaks and atoms previously labelled as water
6	6*	53.8	20.2	Arg42 removed, two waters added
7	4*	53.2	20.1	Disorder at Arg42, Glu7, Arg53 added, water rebuilt, erroneous restraint fixed
7	24†	46.2	17.5	H atoms added, absorption correction, non-disordered atoms made anisotropic
9	50†	37.6	12.7‡§	Water structure rebuilt, disorder and restraints checked after batches of ten cycles each

* Blocked full-matrix refinement (β-test version of *SHELXL*92). † Conjugate-gradient refinement (γ-test version of *SHELXL*92 and release version *SHELXL*93). ‡ After round 9, various parts of the structure were selectively rebuilt from 'omit' maps. The anisotropic model converged with $R = 12.2\%$ [$F > 4\sigma(F)$, 16.1% on all data]. An isotropic model converged with $R = 14.6\%$ [$F > 4\sigma(F)$, 18.7% on all data]. § Overall deviations of the model from the 'ideal' values of Engh & Huber (1991) are 0.035 Å and 3.1° for bond lengths and angles respectively.

At the end of anisotropic refinement, the R factor was 12.2%. Thermal parameters were then converted back to their isotropic equivalents and the model underwent numerous cycles of least-squares refinement and rebuilding from 'omit' maps. It eventually reached convergence with a conventional R factor [based on $F > 4\sigma(F)$] of 14.6%. An overview of the stages in the rebuilding/refinement process which led to a complete model are given in Table 2.

3. Results

3.1. *Overall features*

There are a number of differences between the model obtained in this refinement and the models obtained from room-temperature data. The cell dimensions observed at 125 K were noticeably different from those at room temperature. The overall decrease in cell volume of about 3% on cooling to 125 K is normal for molecular crystals, and has been observed in crystals of other proteins such as crambin (Hope, 1988; Parkin, 1993; Parkin & Hope,

1993), sperm whale metmyoglobin (Hartmann *et al.*, 1982), and concanavalin A (Parkin, 1993; Parkin & Hope, 1993). This reduction, however, belies the true extent of the difference. At 125 K, the *a* axis was observed to be longer than at room temperature: 75.39 (3) Å as compared to 74.1 Å. Both the *b* and *c* axes were shorter at 125 K than at room temperature: 22.581 (7) and 28.606 (9) Å for *b* and *c*, respectively, compared to 23.4 and 28.9 Å. These disproportionately large changes hinted at the likelihood of significant differences between the structures at 125 K and room temperature.

3.2. *Secondary structure*

The overall secondary structure obtained at 125 K follows the same general form as that observed at room temperature, which in turn is very close to that found for form I crystals of BPTI (Huber *et al.*, 1970; Deisenhofer & Steigemann, 1975) and form III crystals (Wlodawer *et al.*, 1987). A Ramachandran plot (not shown) was unremarkable, there were no significant deviations of dihedral angles from the allowed regions. The only substantial difference in the backbone trace is at residues Gly56, Gly57 and Ala58, for which unambiguous electron density was not found using room-temperature X-ray diffraction data in 5PTI (Wlodawer *et al.*, 1984*b*) or 9PTI (Eigenbrot *et al.*, 1991). The ψ torsional angle of Gly56 from this refinement is $-2°$ compared to about $-160°$ at room temperature (see Table 3), showing that residues Gly57 and Ala58 occupy a quite different region of space than those indicated (albeit weakly) at room temperature. In the room-temperature structure of a Tyr35Gly mutant (8PTI) in space group $P4_22_12$ (Houssett *et al.*, 1991*b*), good electron density was obtained at the C-terminus, but not in positions that correlate with any of the native structures thus far reported, including this low-temperature model.

Close to the amino terminus of BPTI, there is a short 1.5 turn region of 3_{10} helix formed by residues Asp3 to Glu7. This is connected to a more substantial α-helix composed of residues Ser47 to Gly56 by a disulfide bridge between Cys5 and Cys55. A disulfide bridge between Cys30 and Cys51 joins the α-helix to the main body of the protein, which is a double-stranded antiparallel β-sheet made up of residues Ala16 to Asn24 and Gly28 to Gly36, joined by a loop formed by residues Ala25, Lys26 and Ala27. This β-sheet is augmented by Thr11 and Phe45, which are hydrogen bonded to Tyr35 and Tyr21, respectively. A hydrogen bond between the backbone N atom of Asn44 and the carboxyl O atom of Arg42 produces a sharp turn with the geometry of a 2_7 ribbon structure (Wlodawer *et al.*, 1984*a*). The secondary structure is completed by loops at residues Gly12 to Lys15 and by Gly37 to Ala40, which are joined through a disulfide bridge between Cys14 and Cys38.

Table 3. *Comparison of φ and ψ (°) for Gly56, Gly57 and Ala58 of various BPTI studies*

	φ_{55}	ψ_{55}	φ_{56}	ψ_{56}	φ_{57}	ψ_{57}
This work	−115.9	−15.2	−82.1	2.0	87.0	−172.0
5PTI	−113.9	−15.9	−88.1	−167.2	−163.8	−138.1
9PTI	−111.3	−8.2	−89.7	−167.1*	−175.8*	−155.7*
	—	—	—	157.7†	−176.1†	−152.3†
8PTI	−118.8	−15.5	−47.8	133.3	87.4	−4.3

* Part *a* of the disorder model used in 9PTI. † Part *b* of the disorder model used in 9PTI.

3.3. *Thermal parameters*

The average backbone *U* values are greatly reduced at 125 K (Fig. 1*a*) and correlate well with the observed secondary structure. The thermal parameters of the backbone atoms of residues Ala16 to Gly36 are all quite low, but there is a slight increase at the residues which form the kink. Regions around Thr11 and Phe45 show relatively low thermal motion, presumably as a result of

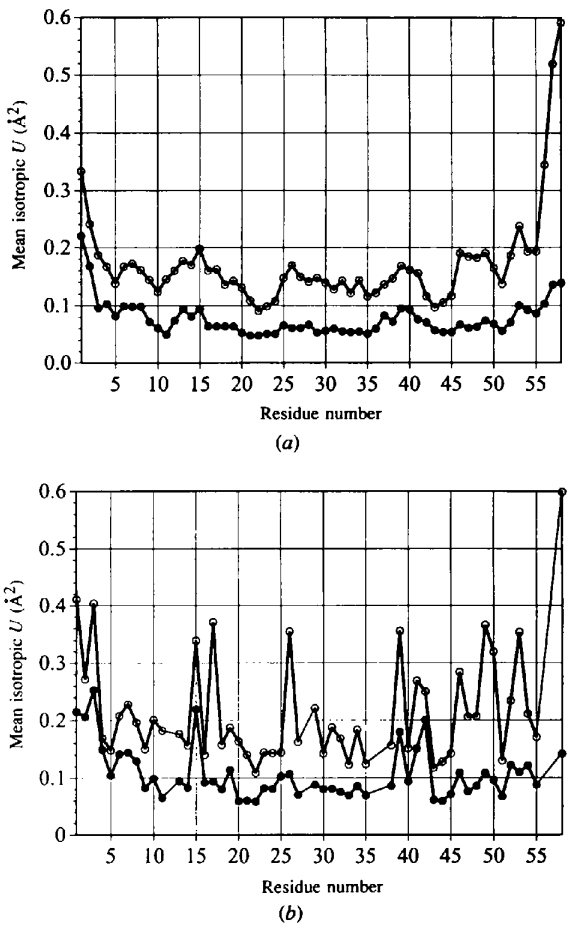

Fig. 1. Thermal parameters *versus* residue number for BPTI form II crystals at 125 K (filled circles, this work) and room temperature (open circles, 5PTI). (*a*) Backbone atoms; (*b*) side-chain atoms.

their association with the β-sheet. There is a dip in thermal parameters at each of the three disulfide linkages (except for Cys30). The backbone atoms of the two floppy loop regions from Gly12 to Lys15 and Gly37 to Ala40 have thermal parameters that are higher than average. Residues Arg1, Pro2 and Asp3 at the amine terminus and Gly56, Gly57 and Ala58 at the carboxyl terminus undergo the greatest thermal motion. Thermal parameters for side-chain atoms (Fig. 1*b*) are also much smaller at 125 K compared to room temperature. Those of residues Arg17, Lys26, Lys46, Glu49, Asp50, Arg53 and Ala58 are much smaller, by a factor that is larger than would be expected from just the temperature reduction (Hope, 1988; Hartmann *et al.*, 1982).

3.4. *Solvent structure*

A total of 145.6 water molecules, spread over 167 sites, and two half-occupancy phosphate anions were included in the final model. On density considerations, these account for more than 90% of the expected solvent. There are four water molecules enveloped within the protein; their positions are in complete agreement with those found at room temperature for internal water in all three forms of native BPTI crystals. About two thirds of the water is in the first hydration shell, hydrogen bonded to both the BPTI molecule and to other waters. The rest is in the second and higher solvation shells, hydrogen bonded only to other water molecules or to phosphate. These water molecules exhibit higher thermal motion and a greater degree of disorder. There are 123 water molecules modelled at full occupancy, and 39 sites are modelled at half occupancy. The proximity of all but one of these half-occupancy waters to other electron-density features shows that they are necessarily disordered, but no attempt was made to refine their partial occupancies. The remaining water molecule was modelled at half occupancy due to the sizes of its electron density (too low) and thermal parameter (too high) when refined at full occupancy. In addition, disorder at Glu7 and Arg53 forces one and two water sites, respectively, to the occupancy factor of the major side-chain component. The only other notable feature in the solvent region is composed of two overlapping spheroids 1.45 Å apart with roughly equal dimensions, but unequal electron density. It was modelled as two water sites with fixed occupancy factors 0.8 and 0.2 and refined thermal parameters of about $B = 6.0\,\text{Å}^2$ ($U = 0.075\,\text{Å}^2$). The lower occupancy site makes a contact of 2.99 Å with C_ε of Met52, though there was no unaccounted for electron density around the S_δ atom to construct a disorder model for the C_ε atom. No overwhelming evidence for a counter cation could be found. It is possible that such a cation would disorder over different sites in the crystal, or its position could have been assigned to one or more of the water molecules.

Hydrogen-bonded water molecules surrounding hydrophobic side chains form ring structures similar to those found in crambin (Teeter, 1984) but almost as many are hexagonal as are pentagonal (Fig. 2). Some polar and charged groups exposed on the surface of the protein are also involved in these ring structures.

The beneficial effects of low temperature are readily apparent when compared to room-temperature work. In

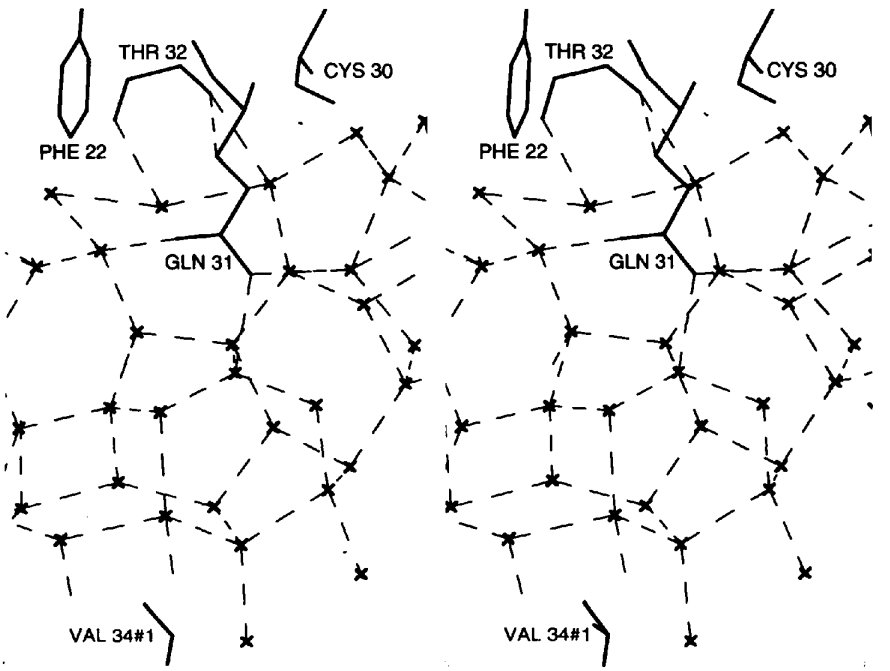

Fig. 2. Stereoview (cross-eye) of hydrogen-bonded water structures at 125 K. Note the presence of both 5 and 6 membered rings. Symmetry code 1: $\frac{1}{2}+x, y-\frac{1}{2}, -z$.

the refinement by Wlodawer *et al.* (1984*a*,*b*), 63 water solvent sites (29 at full occupancy) and a single phosphate position were identified. Eigenbrot *et al.* (1991), reported 67 water sites (51 at full occupancy) and two half-occupancy phosphates. The increased clarity of electron-density maps at low temperature can undoubtedly play a major role in easing the burden of water structure interpretation (see Figs. 3*a*,*b*).

3.5. *Disorder*

In the final model of BPTI from this refinement, only two of the residues, Glu7 and Arg53 (Figs. 4*a* and 4*b*)

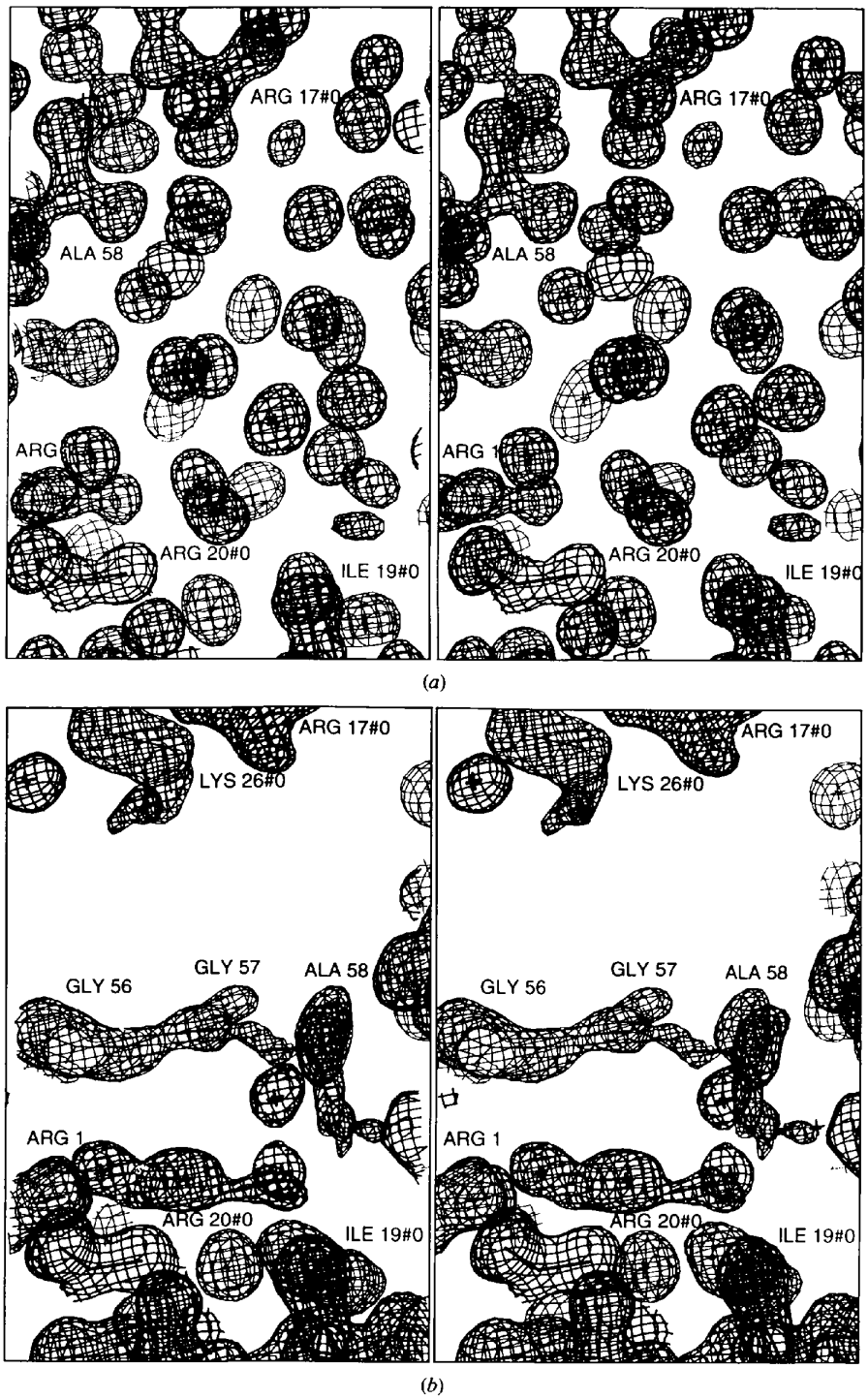

Fig. 3. Stereoview (cross-eye) of electron density contoured at the 1.0σ level (coefficients F_{obs}) in the solvent region near the carboxyl terminus at (*a*) 125 K (this work), and (*b*) room temperature (5PTI). Symmetry code 0: $\frac{1}{2}-x, -y, \frac{1}{2}+z$.

have disorder modelled explicitly over two sites with refined occupancy factors. The side chains of residues Asp3, Lys15, Arg39 and Arg42, however, have thermal parameters that show signs of either multiple conformations or large vibrational amplitudes. Neither the resolution nor the quality of the data allowed any electron density from alternative conformations to be located unambiguously for these residues. Eventually, after much adjustment and rebuilding of side chains using 'omit' maps, the thermal parameters were allowed to accommodate these effects.

It is surprising that only a single conformation was required to model residues Gly57 and Ala58, as they have consistently defied location in room-temperature work. In previous X-ray studies, no convincing electron density had been observed for these residues (Figs. 5*a*,*b*), and only a weak suggestion of their position was given by neutron diffraction (Wlodawer *et al.*, 1984*a*). In another high-resolution study at 1.22 Å (Eigenbrot *et al.*, 1991), Gly57 and Ala58 were modelled in two conformations, one of which corresponded quite closely to the positions indicated weakly by neutron diffraction. Neither conformation, however, was particularly well defined in view of the large thermal parameters attached to the fractional occupancy atoms. None of the previously reported configurations for Gly57 and Ala58 are in agreement with those given here.

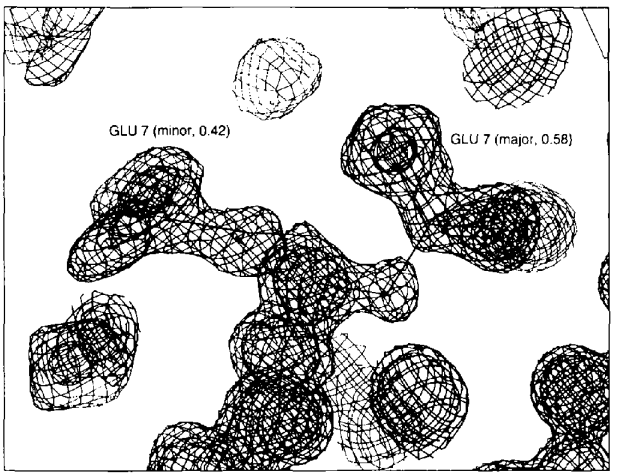

(*a*)

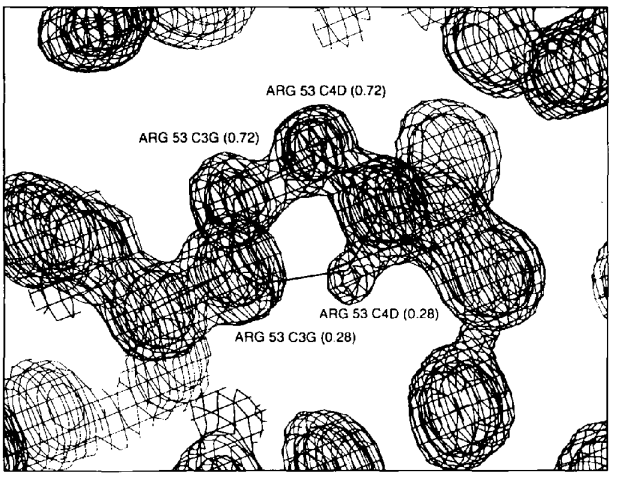

(*b*)

Fig. 4. Electron densities contoured at 1.0σ and 0.5σ (coefficients F_{obs}) at the two residues (*a*) Glu7 and (*b*) Arg53 for which refined disorder models were included.

Table 4. *Intermolecular hydrogen bonds*

Intermolecular contact	This work (Å)	5PTI (Å)	9PTI (Å)
N Arg17···O Ala25^{i}	3.00	3.09	3.02
N_{ε} Arg17···$O_{terminal}$ Ala58^{ii}	2.76	*†	*†
$N_{\eta 1}$ Arg17···O 58 (ii)	2.79	*†	*†
$N_{\eta 2}$ Arg17···$O_{\varepsilon 2}$ Glu49^{iii}	2.90	*‡	*‡
O_{η} Tyr21···O Ala27^{iii}	2.73	3.03	3.01
O_{η} Tyr21···O Gly28^{iii}	3.31	3.28	3.24
$N_{\eta 1}$ Arg39···O Asn44^{iv}	3.09	3.04	3.10, (4.28)§
$N_{\eta 2}$ Arg39···O Asn44^{iv}	3.17	3.23	3.45, (6.31)§

Symmetry codes: (i) $x, y, z+1$; (ii) $x, y-1, z+1$; (iii) $-x+\frac{1}{2}, -y+1, z+\frac{1}{2}$; (iv) $-x+1, y-\frac{1}{2}, -z+\frac{1}{2}$.
* Side chain of Arg17 is given in a different conformation at room temperature. † Ala58 is in a different conformation at room temperature. ‡ Side chain of Glu49 is given in a different conformation at room temperature. § Minor part of 9PTI Arg39 side chain is given in a different conformation.

3.6. *Intermolecular hydrogen bonds*

There are eight intermolecular contacts at 125 K that show evidence of hydrogen-bonding interactions (see Table 4). Three of these are not represented in either 5PTI or 9PTI as they involve contacts between the side-chain N atoms N_{ε} and $N_{\eta 2}$ of Arg17 and the C-terminal O atoms of Ala58 and between $N_{\eta 1}$ of Arg17 and $O_{\varepsilon 2}$ of Glu49. In 9PTI, the major conformer (0.70) of the Asn44 side chain is in rough agreement with both 5PTI and the models from this low-temperature refinement, while the minor component is not. On average, equivalent intermolecular contacts are about 3% shorter at 125 K than those at room temperature.

4. Discussion

4.1. *Accuracy and precision*

As with the majority of protein structure determinations, a proper analysis of accuracy and precision in this refinement of BPTI is made difficult by the lack of true estimated standard deviations. Some indication of the upper bounds of coordinate errors can be obtained from a Luzzati plot (Luzzati, 1952), which charts the variation in R factor with data resolution (Fig. 6). The upper bound coordinate error suggested by the plot is about 0.12 Å, but this value must be treated with caution as the Luzzati plot can overestimate errors, presumably because it assumes that all variations in R factor stem from coordinate errors (Guss, Bartunik & Freeman, 1992;

Parkin, 1993), which is certainly not the case. True deviations from reality are likely to depend on the local environment, being smaller in the better defined regions of the protein. In the absence of a second (independent) low-temperature refinement for direct comparison, we compare root-mean-square (r.m.s.) deviations of atomic positions between isotropic and anisotropic refinements against the low-temperature data, and with the two available room temperature models (5PTI and 9PTI).

4.2. *Comparison of isotropic and anisotropic models at low temperature*

The data-to-parameter ratio of 3.6:1 resulting from restrained anisotropic treatment of thermal parameters, puts such a refinement of BPTI on the borderline of feasibility. In most protein structure refinements, the attainable resolution of data is much lower, so that refinement of only atomic coordinates and isotropic thermal parameters can give similar (or much worse!) data-to-parameter ratios. Observations from small-molecule refinements suggest that atomic coordinate differences between isotropic and anisotropic refinements are often negligible (Parkin, 1993; Parkin & Hope, 1994). All anisotropic thermal parameters from the final model were first converted to their isotropic equivalents. The model was then subjected to several rounds of 'omit' map rebuilding and least-squares refinement to remove as much of the memory of the anisotropic model as was practicable. For the whole contents of the asymmetric unit, the r.m.s. difference in atomic coordinates (mapped one to one) was 0.086 Å. In more specific regions of the structure, the r.m.s. deviations showed the expected trends. In the BPTI molecule alone, the r.m.s. deviation is 0.057 Å, which can be subdivided into 0.048 Å for the ordered groups and 0.123 Å for disordered groups. Differences in the side chains (0.070 Å) are larger than those in the backbone (0.040 Å). Coordinate differences in the solvent and phosphate regions are higher than those in the protein molecule. For all the water and phosphate combined, the r.m.s. deviation is 0.135 Å. For the full occupancy water it is lower, at 0.101 Å, and for the disordered water and phosphate, it is 0.192 Å.

The small changes in structural parameters between isotropic and anisotropic models compare favourably with those found in separate refinements (both using identical data and isotropic temperature factor models, but different program systems) of poplar plastocyanin at 173 K (Fields *et al.*, 1994). The r.m.s. deviation for the backbone atoms of this protein at the somewhat lower resolution of 1.6 Å, was 0.086 Å. Deviations of the same order of magnitude were also obtained in separate refinements against F and F^2 (derived from the same experimental set) of ribonuclease A by Harris & Moss (1992). These numbers suggest that the characteristics of the program used, the relative strengths of restraints, weighting schemes, use of F or F^2, operator subjectivity *etc.*, can play at least as important a role as the temperature-factor model in determining how the least-squares process (possibly combined with other optimization schemes such as simulated annealing) adjusts the parameters that are identified as 'atomic positions'.

These small structural parameter differences are in stark contrast to the large drop in R factors that accompanied the modelling of anisotropic motion. To investigate whether the more demanding refinement strategy actually led to an improved model, we have used Brünger's R(free) statistic (Brünger, 1992, 1993) to provide an estimate of model quality and residual phase error. For R(free) to be statistically valid, the subset of data excluded from use in refinement must truly represent the full data set, *i.e.* it must be a random sample. In *SHELXL92/3* (Sheldrick, 1992, 1993), the data subset is created by omission of every nth reflection, where n is typically about 10. Since this need not produce a truly random sampling, we have calculated a weighted average R(free) from data subsets with $n = 9$, 10 and 11. This approach has the added advantage of allowing us to give an uncertainty associated with the statistic. Prior to the refinement cycles needed to calculate R(free), the conventional R factors based on all data were 16.2 and 19.0%, respectively, for the models with anisotropic and isotropic thermal parameters. R factors calculated from the three data subsets used for R(free) estimation prior to further refinements were 16.0 (5) and 18.9 (4)%, confirming that the weighted average R(free) did indeed properly represent the full data set. Individual quantities for each of the three data subsets are given in Table 5. For each R(free) calculation, 50 cycles of conjugate-gradient refinement with *SHELXL93* (Sheldrick, 1993) were performed after a 'coordinate shake' (r.m.s. deviation 0.18 Å) to remove the memory effect inherent to non-centrosymmetric problems, and to ensure proper convergence. For the isotropic model, we obtained an R(free) of 21.8 (4)% and for the anisotropic model it was 21.5 (5)%. Since there is no statistically significant difference between these quantities, we conclude that anisotropic refinement was not warranted in this case as it did not lead to a more accurate model. This is despite the reduction in the conventional R factor by nearly three percentage points, and is in complete accord with the small differences observed in atomic positions before and after anisotropic thermal parameters were introduced.

4.3. *Comparison of room- and low-temperature structures of BPTI*

The backbone trace from Arg1 to Cys55 is little different at 125 K from that at room temperature. The r.m.s. deviations between refinements for backbone atoms are given in Table 6. For the C_α atoms of these amino acids it is 0.39 and 0.37 Å in comparison with 5PTI (Wlodawer *et al.*, 1984*a*,*b*) and 9PTI (Eigenbrot *et*

al., 1991), respectively. Residues Gly56, Gly57 and Ala58, however, are markedly different at 125 K, where unambiguous electron density for all atoms was found with no particular problem (Figs. 5*a* and 5*b*). In fact, the atomic positions of Gly56, Gly57 and Ala58 were found in a difference map by a peak-picking routine in *SHELXL92* rather than by visual analysis of electron-density maps. In the present refinement, discrete modelling of disorder over more than one site was only necessary for Glu7 and Arg53 (see Figs. 4*a* and 4*b*). At room temperature, disorder appears to have been much more of a problem. In 9PTI, the side chains of Asp3, Glu7, Arg39, Arg42, Glu49, Asp50, Met52 and Arg53 were modelled over two sites. Less disorder was modelled in 5PTI, though analysis of thermal parameters suggests that there could have been more disorder than was explicitly modelled. It is of course possible that some disorder is present at 125 K but not represented in our model. In particular, the side chains of Asp3, Lys15, Arg39 and Arg42 have rather large thermal parameters,

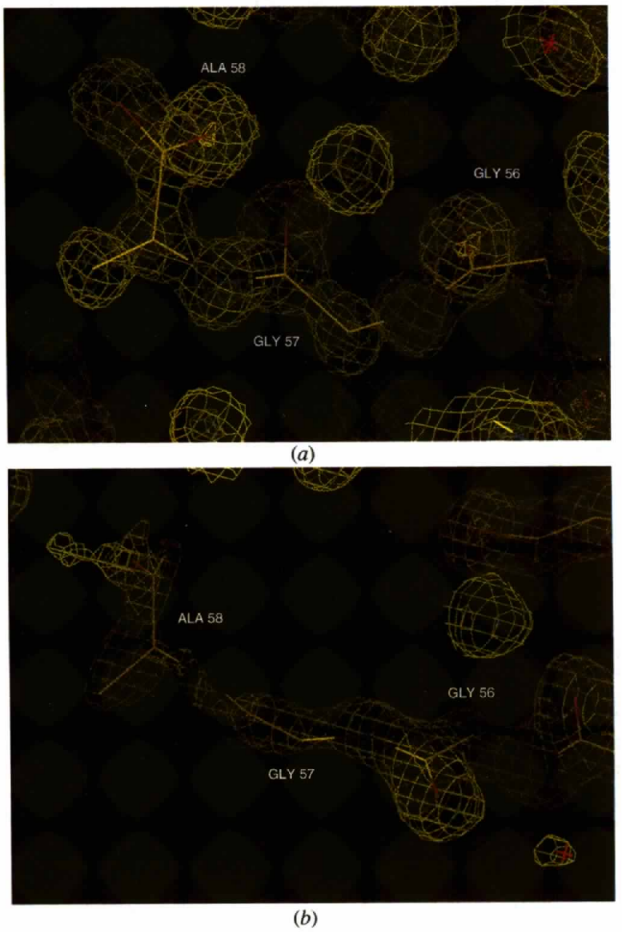

Fig. 5. Electron densities contoured at 1σ, 3σ and 5σ (coefficients F_{obs}) for the carboxyl-terminal residues Gly56, Gly57 and Ala58 at (*a*) 125 K (this work), and (*b*) room temperature (5PTI and R5PTISFX.Z).

Table 5. *Values of R and R(free) before and after refinement runs used to calculate R(free)*

	'Isotropic' before	'Anisotropic' before	'Isotropic' after	'Anisotropic' after
R_1 (all data)	0.190	0.162	0.191	0.164
R_1(free), $n = 9$*	0.185	0.155	0.213	0.209
R_1(free), $n = 10$*	0.190	0.164	0.220	0.220
R_1(free), $n = 11$*	0.192	0.162	0.221	0.215
R_1(free), ave.	0.189 (4)	0.160 (5)	0.218 (4)	0.215 (5)
wR_2 (all data)	0.422	0.362	0.426	0.371
wR_2(free), $n = 9$*	0.412	0.346	0.480	0.475
wR_2(free), $n = 10$*	0.428	0.366	0.496	0.494
wR_2(free), $n = 11$*	0.423	0.366	0.492	0.489
wR_2(free), ave.	0.421 (8)	0.359 (11)	0.489 (8)	0.485 (10)

* The reflection subset used to calculate R(free) was created from every nth reflection.

Table 6. *Root-mean-square differences between BPTI backbones*

Low-temperature r.m.s. differences were calculated straight from the atomic coordinates, but those between low/room and room/room models were calculated following the method described by Kearsley (1989), in order to maximize the overlap.

	N, C_α, C, O (Å)	C_α only (Å)
125 K iso/aniso (this work)	0.040	0.039
125 K iso*/5PTI (1–55)†	0.32	0.39
125 K iso*/9PTI (1–55)†	0.32	0.37
5PTI/9PTI (1–55)†	0.17	0.072

* Results for the anisotropic low-temperature model were not significantly different. † Quantities are for Aeg1–Ala55 due to the difference in ψ torsional angle of Gly56 at low and room temperatures.

in comparison to their neighbours (Fig. 1*b*). There is no unaccounted-for electron density in these regions, however (Figs. 7*a*–7*d*), and the separation of disordered components would be too small to justify split-atom refinement.

In addition to Gly57 and Ala58, various side chains were found in quite different positions at low temperature. In particular, Met52, which was oxidized in 9PTI

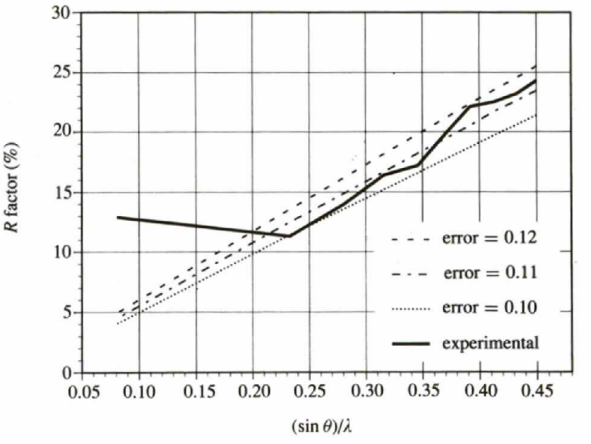

Fig. 6. Luzzati plot (Luzzati, 1952) for the refinement at 125 K.

(Eigenbrot *et al.*, 1991) and modelled as disordered over two positions in both room-temperature studies, was found unoxidized, in a single orientation at 125 K. The side chains of residues Thr11, Arg17, Glu49, Asp50 and Arg53 were also found in different places in this refinement. With the exception of Thr11, these all have rather large thermal parameters. At room temperature, disorder had been modelled over two sites of Glu49, Asp50 and Arg53 by Eigenbrot *et al.* (1991).

The spontaneous resolution of disorder that occurs in form II crystals of BPTI is possibly related to a minor phase transition during cooling. Some form of rearrangement within the crystal was apparent even before refinement, from the observed lengthening of the *a* axis from 74.1 to 75.39 Å after cooling. If the transition to a more ordered state is truly a consequence of the cooling process, then variations in crystal-cooling techniques may represent an effective mean: of decreasing disorder and hence increasing the attainable resolution. This is, of course, a double-edged sword, as it is also reasonable to argue that a room-temperature structure has more biological relevance. Recent work on poplar plastocyanin at 173 K (Fields *et al.*, 1994) revealed a 'peptide flip' in a turn region which apparently occurred as a result of cooling. Preliminary work on concanavalin A has identified a minor phase transition at about 165 K (Parkin, 1993; Parkin & Hope, 1993). Whether this is associated with rearrangement to a more ordered state is still under investigation.

5. Concluding remarks

Refinement of BPTI against low-temperature X-ray diffraction data has resulted in a structure with a higher information content than the refinements against room-temperature data reported previously. Even though the data were relatively weak in terms of counting statistics (especially at high angle), electron-density maps were very clear and allowed unambiguous location of residues Gly57 and Ala58 that had not been reliably observed at

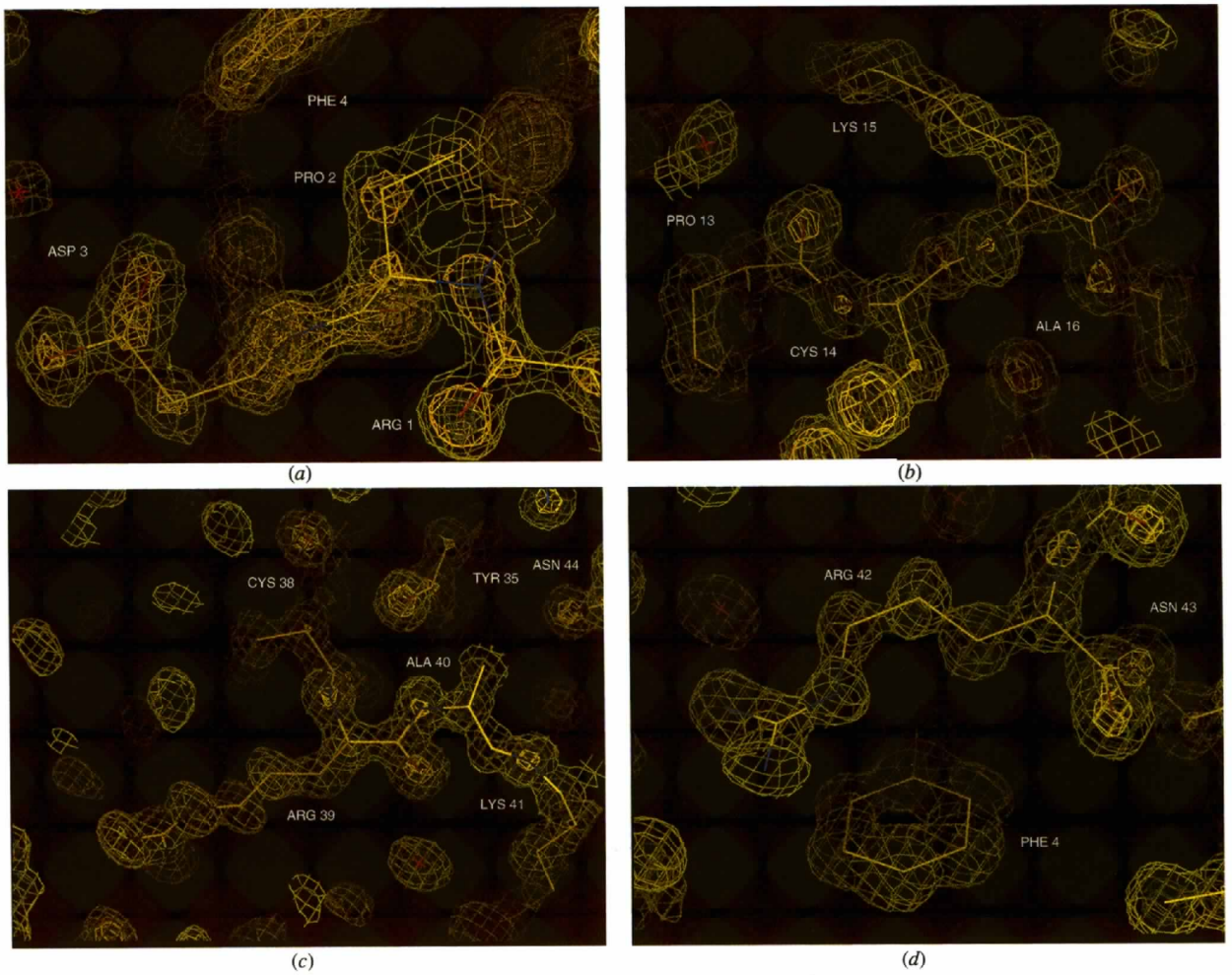

Fig. 7. Electron densities contoured at 1σ, 3σ and 5σ (coefficients F_{obs}) in regions with high refined thermal parameters at 125 K, the side chains of residues (*a*) Asp3, (*b*) Lys15, (*c*) Arg39 and (*d*) Arg42.

room temperature. The number of side chains that required modelling over multiple sites was reduced, and although substantial rebuilding in some parts of the molecule was necessary, refinement proceeded quite smoothly. A comparison of models with anisotropic and isotropic thermal parameters showed only small adjustments to atomic coordinates when the more sophisticated model for atomic vibrations was included. This bodes well for protein crystallography, as it is unusual for protein crystals to diffract well enough to support the extra parameters required to refine anisotropic temperature factors. The final conventional R factors of 14.6 and 12.2% [based on $F > 4\sigma(F)$] and 18.7 and 16.1% (based on all data) for isotropic and anisotropic models, respectively, compare favourably with those from room-temperature refinements of BPTI, which have consistently been in the range 16–20%.*

The beneficial effects of lowering the temperature for data collection cannot be stressed too highly. Since most protein crystals can be cooled successfully, substantial increases in the quality of reported structural models are anticipated if low-temperature methods become more common.

We are grateful to Professor Wayne Hendrickson for the form II crystals of BPTI used in this work and to Dr Karl Weisgraber for constructive criticism of the manuscript. SP would like to thank the Regents of the University of California, for the award of a Regents Fellowship. Part of this work was performed under the auspices of the US Department of Energy at Lawrence Livermore Laboratory under contract No. W-7405-ENG-48.

* Atomic coordinates and structure factors have been deposited with the Protein Data Bank, Brookhaven National Laboratory (Reference: 1BPI). Free copies may be obtained through The Managing Editor, International Union of Crystallography, 5 Abbey Square, Chester CH1 2HU, England (Reference: AM0026).

References

Bernstein, F. C., Koetzle, T. F., Williams, G. J. B., Meyer, E. F. Jr, Brice, M. D., Rodgers, J. R., Kennard, O., Shimanouchi, T. & Tasumi, M. (1977). *J. Mol. Biol.* **112**, 535–542.

Brooks, B. & Karplus, M. (1983). *Proc. Natl Acad. Sci. USA*, **80**, 6571–6575.

Brünger, A. T. (1992). *Nature (London)*, **355**, 472–475.

Brünger, A. T. (1993). *Acta Cryst.* D**49**, 24–36.

Dauter, Z., Sieker, L. C. & Wilson, K. S. (1992). *Acta Cryst.* B**48**, 42–59.

Deisenhofer, J. & Steigemann, W. (1975). *Acta Cryst.* B**31**, 238–250.

Diamond, R. (1971). *Acta Cryst.* A**27**, 436–452.

Driessen, H., Haneef, M. I. J., Harris, G. W., Howlin, B., Khan, G. & Moss, D. S. (1989). *J. Appl. Cryst.* **22**, 510–516.

Eigenbrot, C., Randal, M. & Kossiakoff, A. A. (1991). Protein Data Bank entry PDB9PTI, Brookhaven National Laboratory, Upton, NY., 11973, USA.

Engh, R. A. & Huber, R. (1991). *Acta Cryst.* A**47**, 392–400.

Fields, B. A., Bartsch, H. H., Bartunik, H. D., Cordes, F., Guss, J. M. & Freeman, H. C. (1994). *Acta Cryst.* D**50**, 709–730.

Glover, I., Haneef, I., Pitts, J., Wood, S., Moss, D., Tickle, I. & Blundell, T. (1993). *Biopolymers*, **22**, 293–304.

Guss, J. M., Bartunik, H. D. & Freeman, H. C. (1992). *Acta Cryst.* B**48**, 790–811.

Harris, G. W. & Moss, D. S. (1992). *Acta Cryst.* A**48**, 42–45.

Hartmann, H., Parak, F., Steigemann, W., Petsko, G. A., Ringe-Ponzi, D. & Frauenfelder, H. (1982). *Proc. Natl Acad. Sci. USA*, **79**, 4967–4971.

Hope, H. (1988). *Acta Cryst.* B**44**, 22–26.

Hope, H. & Nichols, B. G. (1981). *Acta Cryst.* B**37**, 158–161.

Housset, D., Kim, K.-S., Fuchs, J., Woodward, C. & Wlodawer, A. (1991*a*). *J. Mol. Biol.* **220**, 757–770.

Houssett, D., Kim, K.-S., Fuchs, J., Woodward, C. & Wlodawer, A. (1991*b*). Protein Data Bank entry PDB8PTI, Brookhaven National Laboratory, Upton, NY., 11973, USA.

Huber, R., Kukla, D., Rühlmann, A., Epp, O. & Formanek, H. (1970). *Naturwissenschaften*, **57**, 389–392.

Kearsley, S. K. (1989). *Acta Cryst.* A**45**, 208–210.

Langridge, R., Marvin, D. A., Seeds, W. E., Wilson, H. R., Hooper, C. W., Wilkins, M. H. F. & Hamilton, L. D. (1960). *J. Mol. Biol.* **2**, 38–64.

Levitt, M. (1981). *Nature (London)*, **294**, 379–380.

Levitt, M. (1983). *J. Mol. Biol.* **168**, 594–617.

Levitt, M. & Warshel, A. (1975). *Nature (London)*, **253**, 694–698.

Luzzati, V. (1952). *Acta Cryst.* **5**, 802–810.

McRee, D. E. (1992). *J. Mol. Graphics*, **10**, 44–46.

Parkin, S. R. (1993). PhD thesis, University of California at Davis, USA.

Parkin, S. R. & Hope, H. (1993). Am. Crystallogr. Assoc. Meet. Abstract PI20. Albuquerque, NM, USA.

Parkin, S. R. & Hope, H. (1994). Am. Crystallogr. Assoc. Meet. Abstract PM14. Atlanta, GA, USA.

Parkin, S. R., Moezzi, B. & Hope, H. (1995). *J. Appl. Cryst.* **28**, 53–56.

Pierrot, M., Haser, R., Frey, M., Brushci, M., Legall, J., Sieker, L. C. & Jensen, L. H. (1976). *J. Mol. Biol.* **107**, 179–182.

Sheldrick, G. M. (1992). *SHELXL92 Crystal Structure Refinement Program*, β and γ test versions. University of Göttingen, Germany.

Sheldrick, G. M. (1993). *SHELXL93 Crystal Structure Refinement Program, Release Version*. University of Göttingen, Germany.

Takanaga, S. & Scheraga, H. A. (1975). *Proc. Natl Acad. Sci. USA*, **72**, 3802–3806.

Teeter, M. M. (1984). *Proc. Natl Acad. Sci. USA*, **81**, 6014–6018.

Teeter, M. M. & Hendrickson, W. A. (1979). *J. Mol. Biol.* **127**, 219–223.

Walter, J. & Huber, R. (1983). *J. Mol. Biol.* **167**, 911-917.

Watenpaugh, K. D., Sieker, L. C. & Jensen, L. H. (1979). *J. Mol. Biol.* **131**, 509–522.

Wlodawer, A., Nachman, J., Gilliland, G. L., Gallagher, W. & Woodward, C. (1987). *J. Mol. Biol.* **198**, 469–480.

Wlodawer, A., Walter, J., Huber, R. & Sjölin, L. (1984*a*). *J. Mol. Biol.* **180**, 301–329.

Wlodawer, A., Walter, J., Huber, R. & Sjölin, L. (1984*b*). Protein Data Bank entry PDB5PTI, structure-factor entry R5PTISFX.Z, Brookhaven National Laboratory, Upton, NY., 11973, USA.

Wüthrich, K., Wider, C., Wagner, G. & Braun, W. (1982). *J. Mol. Biol.* **155**, 311–319.